Proceedings of the ASME 2014 Dynamic Systems and Control Conference
DSCC2014
October 22-24, 2014, San Antonio, TX, USA

DSCC2014-5988

ON THE STABILITY OF TIRE TORSIONAL OSCILLATIONS UNDER LOCKED-WHEEL BRAKING

Chunjian Wang
Clemson University
Greenville, SC, USA

John Adcox
Clemson University
Greenville, SC, USA

Beshah Ayalew
Clemson University
Greenville, SC, USA

Benoit Dailliez
Centre de Technologie Europe,
Michelin Corporation
Clermont Ferrand, France

Timothy Rhyne
Michelin Americas Research
Corporation
Greenville, SC, USA

Steve Cron
Michelin Americas Research
Corporation
Greenville, SC, USA

ABSTRACT

This paper deals with the stability of self-excited tire torsional oscillations during locked-wheel braking events. Using a combination of torsionally flexible tire-wheel model and a dynamic tire-ground friction model, it is highlighted that the primary cause of unstable oscillations is the 'Stribeck' effect in tire-ground friction. It is also shown analytically that when suspension torsional compliances are negligible, the bifurcation parameters for the local torsional instability include forward speed, normal load and tire radius. In the presence of significant suspension torsional compliance, it is shown that the stability is also affected by suspension torsional stiffness and damping. Furthermore, the tire torsional stiffness becomes an important bifurcation parameter only in the presence of significant suspension compliance. This analysis gives useful insights for the selection of tire sidewall stiffness ranges and their proper matching with targeted vehicle suspensions at the design stage.

1. INTRODUCTION

Anti-lock braking systems (ABS) have been widely used in passenger cars due to their effectiveness in avoiding skidding, helping optimize stopping distances and directional stability. However, ABSs require additional components, such as hydraulic modulators, a pump and wheel speed sensors as well as a well-designed control algorithm, all of which increase the cost of the systems. For this reason, ABSs are still optional in some markets. During hard braking events without ABS, the wheel can lock up, which in addition to loss of the steerability of the tire, may lead to self-excited torsional oscillation. These self-excited torsional oscillations were observed, for example, in measurements of the braking torque and force during locked-wheel braking experiments[1]. These self-excited oscillations may lead to irregular wear of tire [2, 3], reduced ride quality [4] and/or reduced braking performance[5].

Self-excited oscillation is a common phenomenon in many applications involving sliding friction [6, 7]. As an example, in [8], the stability and local bifurcation behavior of a friction oscillator due to exponentially decaying friction have been investigated and used to explain the low frequency groan of brake noise. As opposed to static friction models used in [8], a dynamic friction model was used to study the bifurcation of a single-degree-of-freedom mechanical oscillator in [9]. For tires, the paper [10] studied the self-excited lateral oscillation using a piecewise friction model and attributed the polygonal wear of tire to this oscillation. However, the self-excited torsional oscillation of a tire during locked-wheel braking has not received much attention, partly because of the successful advent of ABS and traction control systems that prevent wheel lock-up. This paper presents a theoretical analysis of the self-excited torsional oscillation under locked-wheel braking in the absence of well-functioning ABSs.

To begin with, the analysis of tire torsional oscillation requires appropriate tire and tire-ground friction models. A rigid wheel model, which is used in most traction/ABS controller derivations, is not suitable because the rigid wheel assumption excludes torsional oscillation. In [11] a simple dynamic tire model involving relaxation length concepts was described and validated. Later on, based on this concept, a Rigid Ring Tire Model [1] was proposed which allows analysis of tire vibrations. With the inclusion of the tire modes from in-plane [1] to out-of-plane [12] evolved the commercial dynamic tire model, known as the SWIFT tire model[13]. The applications of the SWIFT tire model in braking events have included the prediction of the noise component in the wheel angular velocity signal [14, 15], the study of vehicle behavior on uneven roads[16], and tire shimmy analysis [17]. A complex tire dynamic model, known as FTire proposed in recent years [18, 19], incorporates much more degrees-of-freedom to essentially offer similar capabilities. While these sophisticated models represent the state of the art in tire dynamics modeling, we seek an insightful simplification to isolate self-excited oscillations.

As for the tire-ground friction model, Pacejka's $\boldsymbol{\mu - slip}$ friction model [17] is widely used for its good approximation of test data and low computational intensity. However, this friction model is based on steady-state experimental data, and tire torsional oscillation under locked-wheel braking is very much a dynamic phenomenon. In [20], a dynamic tire-ground friction model, which is called Average Lumped Parameter model or simply the LuGre tire model, was presented. This tire-ground friction model includes an internal state which represents the tread dynamics for friction generation. This model and its variants[21, 22] have been found to be quite suitable for analyzing friction induced oscillations in many applications [9, 23-25].

In this paper, we adopt a flexible sidewall tire model [26] which captures the tire torsional oscillation. This is a simplification of Rigid Ring Tire Model to the in-plane torsional dynamics due primarily to tire sidewall torsional flexibility. By coupling this model with the LuGre tire-ground friction model, the stability and local bifurcation of locked-wheel braking events will be analyzed. In addition, the effect of suspension torsional compliance and damping on the stability of the self-excited oscillations will be studied.

The rest of the paper is organized as follows. Section 2 describes the system model adopted. Section 3 details the analysis of the stability and local bifurcation of the system. Section 4 takes a closer look at the 'Stribeck' effect in the tire-ground friction model. In Section 5, the tire torsional oscillation is studied by including a torsionally compliant suspension. Finally, conclusions are given in Section 6.

2. TIRE MODEL ADOPTED FOR ANALYSIS

To focus the analysis on the pure torsional dynamics, the following assumptions are made: We consider one corner of a vehicle, where the vehicle/wheel center is assumed to have a longitudinal velocity$\mathbf{v_v}$ during the locked-wheel braking event. Torsional deformation in the tire is assumed to remain in the linear range so that the tire sidewall torsional stiffness $\mathbf{K_T}$ and damping coefficient $\mathbf{C_T}$ can be taken as constants. The schematic of the flexible sidewall tire model adopted is shown in Figure 1, where $\mathbf{J_r}$ is the inertia of ring/belt of the tire and $\mathbf{F_z}$ is tire normal load.

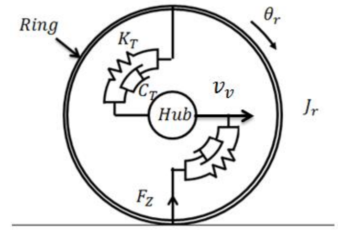

Figure 1: Flexible sidewall tire model

We first consider the case where the wheel/hub is supported on a rigid structure (no suspension compliance). The equation of torsional motion for tire ring is given by:

$$J_r\ddot{\theta}_r = F_Z R\mu - K_T\theta_r - C_T\dot{\theta}_r \tag{1}$$

where R is tire radius and the ground friction coefficient is μ. Note that the wheel/hub is assumed locked with applied braking torque.

The LuGre model computes the friction coefficient by by[20]:

$$\mu = \sigma_0 z + \sigma_1\dot{z} - \sigma_2 v_r \tag{2}$$

where the relative velocity $\mathrm{v_r}$ is

$$v_r = v_v - R\dot{\theta}_r \tag{3}$$

$\sigma_0, \sigma_1$are parameters representing tread stiffness and damping, σ_2 is the viscous damping which is usually very small and can be approximated as 0. z is the internal state representing tread/bristle deflection and its dynamics is given by:

$$\dot{z} = v_r - \frac{\sigma_0|v_r|}{g(v_r)}z - k|\dot{\theta}_r|Rz \tag{4}$$

where

$$g(v_r) = \mu_c + (\mu_s - \mu_c)e^{-\left|\frac{v_r}{v_s}\right|^\alpha} \tag{5}$$

Coefficient $\mathbf{k}$ in (4) is a factor that reflects the tread deflection distribution, and here we adopt the equation from[20]:

$$k = \frac{7}{6} * \frac{1}{L} \tag{6}$$

where L is the length of the contact patch.

During locked-wheel braking, the angular velocity of the ring $\dot{\boldsymbol{\theta}}_\mathbf{r}$ can be assumed relatively small compared with vehicle speed $\mathbf{v_v}$, since high slip ratios are involved in this regime.

$$R|\dot{\theta}_r| < v_v \tag{7}$$

Therefore, according to (3), $\mathbf{v_r}$ will be positive in this regime, and

$$|v_r| = v_r \tag{8}$$

By defining $\boldsymbol{\theta}_\mathbf{r}, \dot{\boldsymbol{\theta}}_\mathbf{r}$ and $\mathbf{z}$ as the states $\mathbf{x_1}, \mathbf{x_2}$ and $\mathbf{x_3}$, the state-space model for the coupled nonlinear system of ground friction and torsionally flexible tire can assembled as the three-state system:

$$\dot{x}_1 = x_2$$

$$\begin{aligned}\dot{x}_2 = &-\frac{K_T}{J_r}x_1 - \left(\frac{C_T}{J_r} + \frac{F_Z R^2\sigma_1}{Jr} - \frac{F_Z R^2\sigma_2}{J_r}\right)x_2 + \frac{F_Z R\sigma_0}{J_r}x_3 \\ &- \frac{F_Z R\sigma_0\sigma_1}{J_r}\frac{(v_v - Rx_2)}{g(v_v - Rx_2)}x_3 \\ &- \frac{F_Z R^2\sigma_1 k}{J_r}|x_2|x_3 + \frac{F_Z R(\sigma_1+\sigma_2)v_v}{J_r} \\ \dot{x}_3 = &-Rx_2 - \sigma_0\frac{v_v - Rx_2}{g(v_v - Rx_2)}x_3 - kR|x_2|x_3 + v_v\end{aligned} \tag{9}$$

where:

$$g(v_v - Rx_2) = \mu_c + (\mu_s - \mu_c)e^{-\left(\frac{v_v - Rx_2}{v_s}\right)^{\alpha}} \tag{10}$$

Equation (9) can be written compactly as:

$$\dot{x} = T(x) \tag{11}$$

where $x = [x_1 \quad x_2 \quad x_3]^T$, and function T is the vector function representing the right hand side in (**9**).

3. STABILITY AND LOCAL BIFURCATION ANALYSIS

For local analysis, we can obtain the equilibrium points of the state space $\{\mathbf{x_0}\}$ by setting the state derivative to zero in (11):

$$\begin{aligned} x_{10} &= \frac{F_Z R g(v_v) - F_Z R\sigma_2 v_v}{K_T} \\ x_{20} &= 0 \\ x_{30} &= \frac{g(v_v)}{\sigma_0}\end{aligned} \tag{12}$$

A state-space model with the origin at the equilibrium can be obtained through simple coordinate transformation:

$$\overline{x} = x - x_0 \tag{13}$$

Write the new state-space model as:

$$\dot{\bar{x}} = F(\bar{x}) \tag{14}$$

The bifurcation surfaces can be found by setting [27]:

$$F(\bar{x}) = 0 \tag{15}$$

$$\frac{\partial F(\bar{x})}{\partial \bar{x}} = J = 0 \tag{16}$$

where J is the Jacobian matrix. The analytical expression for J is given in Appendix I.

In the rest of this section, we study the effect of several parameters such as $\mathbf{R}, \mathbf{F_Z}$ and $\mathbf{K_T}$, as well as vehicle/wheel center velocity $\mathbf{v_v}$, on the stability of the tire torsional oscillation. The nominal values of the pneumatic tire parameters used for illustrations are listed in the Appendix II, some of which are adopted from [26]. It is intuitively expected that higher tire damping $\mathbf{C_T}$ improves the stability, so the analysis will omit discussions of $\mathbf{C_T}$ until Section 5.

3.1 Bifurcation due to v_v

First the vehicle forward speed $\mathbf{v_v}$ will be considered as the bifurcation parameter. Figure 2 shows the locus of eigenvalues of $\mathbf{J}$ when $\mathbf{v_v}$ changes from 10m/s to 5m/s. It can be seen that with the reduction of vehicle speed, a pair of eigenvalues pass through the imaginary axis and their real parts become positive, which indicates a Hopf-bifurcation point [28] where the torsional motion loses its stability. The other eigenvalue is always real and negative, and far from the imaginary axis (bottom of Figure 2). This eigenvalue corresponds to the dynamics of tread/bristle deflection, which converges faster, as should be expected.

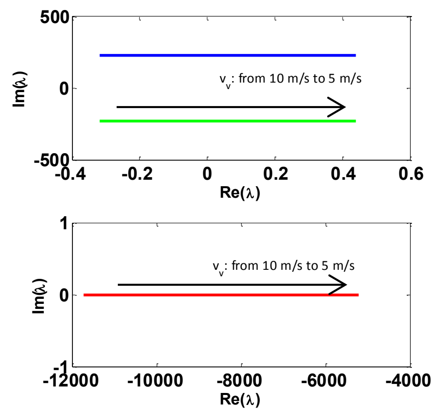

Figure 2: Locus of eigenvalues with changing v_v

Because of the high nonlinearity of $\mathbf{g(v_v)}$ and $\frac{\partial \mathbf{g(v_v - R\bar{x}_2)}}{\partial \bar{\mathbf{x}}_2}$ in the $\mathbf{J}$ matrix, it is difficult to solve the bifurcation point for $\mathbf{v_v}$ analytically. So, a numerical computation is implemented. The bifurcation point of $\mathbf{v_v}$ is found at around $\mathbf{v_v \approx 7.31m/s}$. These results indicate that with the typical parameters listed in Appendix II, the torsion oscillation can be divergent if the vehicle velocity is below 7.3m/s when the wheel/hub is locked.

Figure 3 shows the time history response of θ_r when $v_v = 20m/s$ and $v_v = 1m/s$, respectively. It can be seen the oscillations converge when v_v is above the threshold but diverge when it is below the threshold.

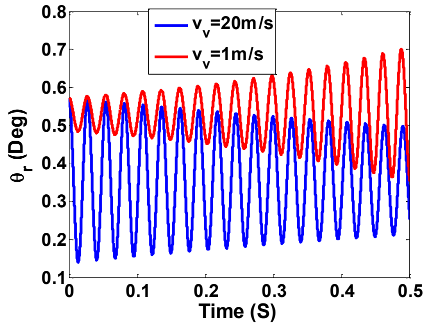

Figure 3: Time response comparison of θ_r for different forward speeds v_v

3.2 Bifurcation surface due to v_v, F_z and R

At a certain vehicle speed $\mathbf{v_v}$, the stability of tire torsional oscillation will also be affected by tire load $\mathbf{F_Z}$ and effective radius $\mathbf{R}$. This bifurcation surface can be obtained by solving (16) for

$$v_v = S(F_Z, R) \tag{17}$$

Figure 4 shows the numerical solution for this surface when $\mathbf{R} \in [\mathbf{0.24m}, \mathbf{0.28m}]$ and $\mathbf{F_z} \in [\mathbf{1000N}, \mathbf{4500N}]$. The bifurcation surface divides the space into stable (above the surface) and unstable (below the surface) areas. It can be seen that the stabilizing $\mathbf{v_v}$ increases with the increase of $\mathbf{R}$ and $\mathbf{F_z}$. This result indicates that with larger radius and higher load, the tire torsional oscillation is more likely to be divergent in locked-wheel braking events from normal vehicle speeds (not necessarily too low speeds).

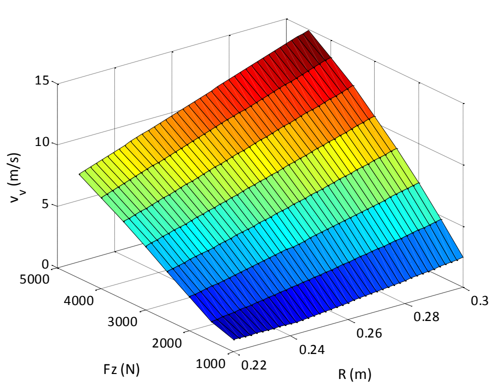

Figure 4: Bifurcation surface of v_v with different R and F_z

3.3 Effect of Tire Torsional Stiffness K_T

With fixed values of $\mathbf{F_Z}$ and $\mathbf{R}$ (at nominal values listed in Appendix II), a relationship between $\mathbf{v_v}$ and $\mathbf{K_T}$ can be solved from (16):

$$v_v = H(K_T) \tag{18}$$

The resulting bifurcation curve from (18) is shown in Figure 5. It can be seen that although in this system the stabilizing $\mathbf{v_v}$ does change with different $\mathbf{K_T}$, the effect is rather small: the difference in the magnitude of the stabilizing $\mathbf{v_v}$ is only about 0.12m/s when $\mathbf{K_T}$ changes from 8000 Nm/rad to 53000 Nm/rad. Further analysis in the next section we will show that this effect of $\mathbf{K_T}$ will disappear if the stead-state tire-ground friction model is used, implying that even this minor effect of $\mathbf{K_T}$ is due to the coupling with tread dynamic friction (since suspension compliances have been ignored so far).

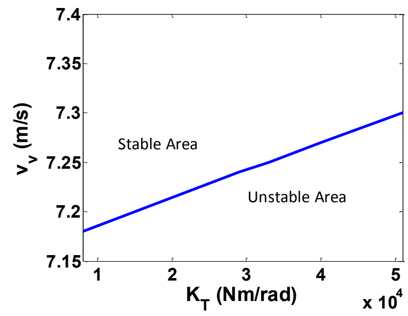

Figure 5: Bifurcation curve in $v_v - K_T$ plane

4. THE STRIBECK EFFECT IN TIRE-GROUND FRICTION

Figure 6 shows the steady state ($\dot{\mathbf{z}} = \mathbf{0}$) $\boldsymbol{\mu} - \mathbf{slip}$ curves obtained from the LuGre model for different vehicle speeds $\mathbf{v_v}$, where slip ratio $\mathbf{s}$ is defined by:

$$s = 1 - \frac{R\dot{\theta}_r}{v_v} \tag{19}$$

It can be seen that in the regime of locked-wheel braking where slip ratio $\mathbf{s} \approx \mathbf{1}$, all the curves have negative slopes. The friction $\boldsymbol{\mu}$ decreases with increase of relative velocity. This negative slope is the so-called the Stribeck effect [29] in the tire-ground friction.

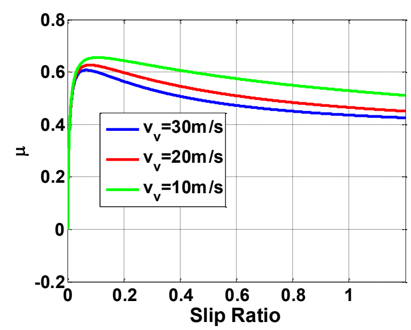

Figure 6: Steady state $\mu - slip$ curves by LuGre model

Denoting the local slope at $\mathbf{s} \approx \mathbf{1}$ by $-\mathbf{p}(\mathbf{v_v})$, at vehicle speed $\mathbf{v_v}$, and the intercept with the $\boldsymbol{\mu}$-axis of a line with this slope $\boldsymbol{\mu}_\mathbf{i}(\mathbf{v_v})$, then the friction coefficient around $\mathbf{s} = \mathbf{1}$ may be represented approximately by:

$$\mu(v_v) = \mu_i(v_v) - p(v_v)s \tag{20}$$

for $|s - 1| \leq \epsilon$, where ϵ is a small constant.

Plugging (20) with (19) into (1), a simplified equation of motion for the ring is obtained:

$$\ddot{\theta}_r = -\frac{K_T}{J_r}\theta_r + \left(\frac{F_Z R^2 p(v_v)}{v_v J_r} - \frac{C_T}{J_r}\right)\dot{\theta}_r + \frac{F_Z R}{J_r}(\mu_i(v_v) - p(v_v)) \quad (21)$$

It is a linear 2nd-order system and the eigenvalues can be obtained analytically:

$$\lambda = \left(\frac{p(v_v)R^2F_z}{2J_r v_v} - \frac{C_T}{2J_r}\right) \pm \frac{\sqrt{-4J_rK_Tv_v^2 + (-p(v_v)R^2F_z + C_Tv_v)^2}}{2J_rv_v} \quad (22)$$

The term under the square root is always negative for reasonable values of vehicle load and forward velocity. Then, it can be seen that when $\mathbf{p(v_v) = 0}$, which means the Stribeck effect is removed, the real parts of the eigenvalues will be always negative, and there will not be unstable oscillation. It is only with a negative slope in $\boldsymbol{\mu} - \mathbf{slip}$ curve, i.e., a positive $\mathbf{p(v_v)}$, that the system can have positive eigenvalues and lose stability when the following condition is satisfied:

$$p(v_v)R^2F_z > C_Tv_v \quad (23)$$

It can be seen from (23) that in the presence of the Stribeck effect, higher tire load and larger tire effective radius will reduce the stability. It can also be concluded that with certain values of these parameters, the oscillation will become unstable if the vehicle velocity $\mathbf{v_v}$ is below a threshold $\frac{\mathbf{p(v_v)R^2F_z}}{\mathbf{C_T}}$.

It can also be noted from (22) that the sidewall torsional stiffness $\mathbf{K_T}$ does not appear in the real part of eigenvalues computed with the steady state friction model. As mentioned above in the discussion of Figure 5 even with dynamic friction, the effect of $\mathbf{K_T}$ on the stability is negligible. However, as will be detailed below, this observation is valid only for the case where suspension torsional compliances are ignored.

5. EFFECT OF SUSPENSION TORSIONAL DYNAMICS

In this section, the wheel/hub will be regarded as supported on torsionally flexible system and the equation for the rotational motion of the hub will be added to the existing model. We assume a linear range of this motion of the hub where the torsional stiffness and damping coefficient of the suspension can be regarded as constants. Figure 7 shows the system model with torsionally flexible suspension and a flexible sidewall tire model.

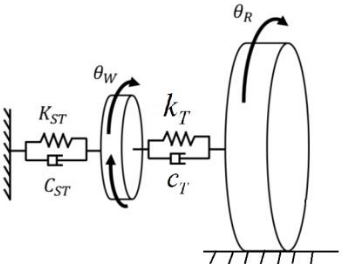

Figure 7: Flexible sidewall tire supported on a torsional flexible suspension

The equation of motion for the ring dynamics is modified to:

$$J_r\ddot{\theta}_r = F_ZR\mu - K_T(\theta_r - \theta_w) - C_T(\dot{\theta}_r - \dot{\theta}_w) \quad (24)$$

with the added dynamics of the hub/wheel:

$$J_w\ddot{\theta}_w = K_T(\theta_r - \theta_w) + C_T(\dot{\theta}_r - \dot{\theta}_w) - K_{ST}\theta_w - C_{ST}\dot{\theta}_w \quad (25)$$

A 5th-order state space model can be assembled combining these equations with the LuGre tire-groud friction model:

$$\dot{x}_s = G(x_s) \quad (26)$$

where the additional states are $x_4 = \theta_w$, $x_5 = \dot{\theta}_w$, x_s is the state vector $x_s = [x_1\ x_2\ x_3\ x_4\ x_5]^T$, and G is the vector function for the right hand side of the 5th order state space model. After coordinate transformation to move the origin to the equilibrium, the Jacobian matrix of this 5th order system J_s is obtained and given in Appendix I.

Using the typical values for $\mathbf{K_{ST}}$ and $\mathbf{C_{ST}}$ listed in Appendix II for a typical suspension for a passenger car, the locus of eigenvalue of the relevant Jacobian for this system is plotted in Figure 8, where $\mathbf{v_v}$ changes from $\mathbf{5m/s}$ to $\mathbf{1m/s}$ (This is even a lower speed range than considered before).

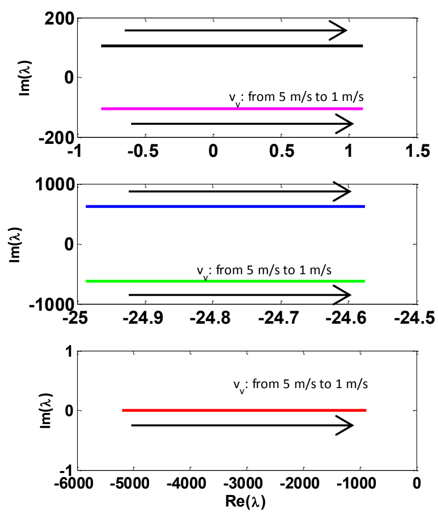

Figure 8: Locus of eigenvalues with suspension torsional flexibility

It can be seen that the Hopf-bifurcation point for $\mathbf{v_v}$ has been reduced from $\mathbf{7.31m/s}$ to $\mathbf{2.39m/s}$, which indicates that the torsional compliance of suspension will help to improve the stability of tire torsional oscillation under locked-wheel braking at normal operating (higher) speeds. Figure 9 shows comparison of the $\boldsymbol{\theta_r}$ response with and without suspension torsional flexibility when $\mathbf{v_v = 5m/s}$. It can be seen that at this vehicle velocity the oscillation becomes convergent with suspension torsional flexibility, which means the stability has been improved. The frequency is also reduced with the presence of suspension torsional flexibility.

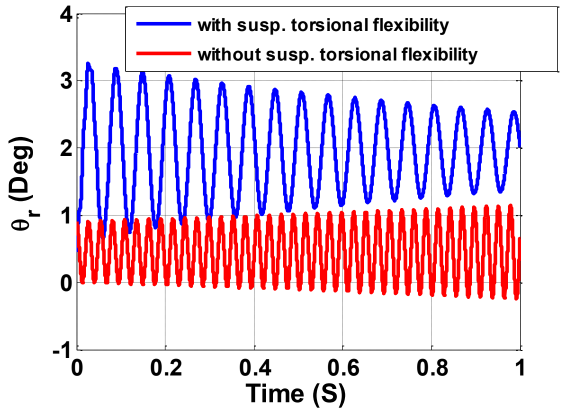

Figure 9: Time response comparison of θ_r with/without suspension torsional flexibility

In particular, the effect of the suspension as well as torsional damping can be seen from the bifurcation surface of $\mathbf{v_v}$ by $\boldsymbol{C_T}$ and $\boldsymbol{C_{ST}}$ as shown in Figure 10, which shows in addition to the intuitive tire torsional damping $\mathbf{C_T}$, the suspension torsional damping $\mathbf{C_{ST}}$ will also help to reduce the stability threshold speed and damp out the tire torsional oscillation. It is also seen in this figure that, increasing $\boldsymbol{C_{ST}}$ is even more effective than increasing $\boldsymbol{C_T}$ in the suppression of the self-excited oscillation. This also means that, with regard to reducing sustained torsional oscillations during locked-wheel braking, high suspension torsional damping values can help to compensate for insufficient torsional damping in tires.

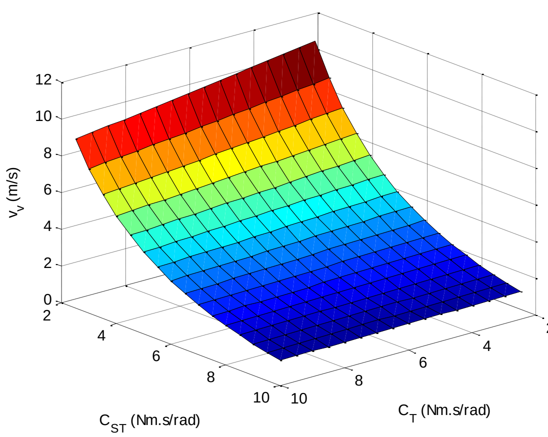

Figure 10: Bifurcation surface of v_v due to C_T and C_{ST}

Another interesting observation is made on the effect of tire torsional stiffness $\mathbf{K_T}$ on the stability of torsional oscillations. It was noted previously that $\mathbf{K_T}$ has a very limited effect on the stability of tire-torsional oscillations in the absence of suspension torsional flexibility. However, the effect of $\mathbf{K_T}$ becomes significant in the presence of suspension torsional flexibility, as shown in Figure 11.

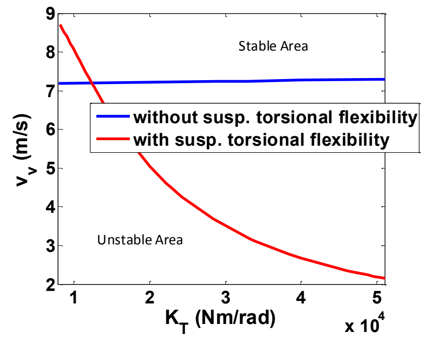

Figure 11: Bifurcation curve in $v_v - K_T$ plane and comparison between systems with/without suspension torsional flexibility

While in the system without suspension torsional flexibility, higher $\mathbf{K_T}$ increases the stabilizing $\mathbf{v_v}$, albeit slightly, making the oscillations 'more unstable'; in the system with suspension torsional flexibility, higher $\mathbf{K_T}$ makes the system more stable in locked-wheel braking at normal forward speeds, pushing the threshold speed much lower. The system without suspension torsional flexibility can be regarded as having an infinite suspension torsional stiffness. From this perspective, the observation can also be restated as: lower suspension torsional stiffness $\mathbf{K_{ST}}$ improves the effect of $\mathbf{K_T}$ on the stability. With an appropriate/realistic choice of $\mathbf{K_{ST}}$, higher $\mathbf{K_T}$ is preferred to improve the stability of tire torsional oscillations. This is also supported by the bifurcation surface of $\mathbf{v_v}$ due to $\mathbf{K_{ST}}$ and $\mathbf{K_T}$, as shown in Figure 12.

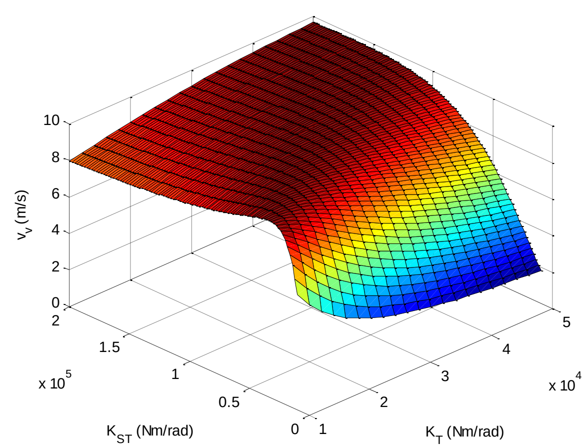

Figure 12: Bifurcation surface of v_v due to K_{ST} and K_T

It can be seen from Figure 12 that to minimize the stabilizing $\mathbf{v_v}$, higher $\mathbf{K_T}$ but lower $\mathbf{K_{ST}}$ is preferred. And in the area with lower $\mathbf{K_{ST}}$, the stabilizing $\mathbf{v_v}$ decreases with increase of $\mathbf{K_T}$; but with higher $\mathbf{K_{ST}}$, this trend reverses. While with higher $\mathbf{K_T}$, the stabilizing $\mathbf{v_v}$ increases with $\mathbf{K_{ST}}$; with low $\mathbf{K_T}$, there will be a value for $\mathbf{K_{ST}}$ beyond which the stabilizing $\mathbf{v_v}$ reaches its maximum value (plateaus) and there is no further improvement to the stability.

6. CONCLUSIONS

The stability of tire torsional oscillation under locked-wheel braking has been analyzed using local bifurcation analysis. The analysis used a combination of the flexible sidewall tire model and dynamic Average Lumped Parameter LuGre tire-ground friction model. It is shown that the self-excited torsional oscillation can be unstable and the instability can be attributed to the Stribeck effect in the tire-ground friction. The bifurcation of the stability can be caused by the combination of the parameters of the forward speed, tire vertical load and tire radius. It is also shown while tire sidewall torsional stiffness has negligible effects on the stability of the oscillation in the absence of a compliant suspension. If the wheel is supported on a torsionally compliant suspension as is generally the case in practice, higher tire torsional stiffness can help improve the stability by lowering the threshold forward speed.

It should be noted that the presented analysis ignored all other compliances and damping that could be coupled to the torsional motion and therefore could damp out or be influenced by the self-excited oscillation. Analysis of these interactions requires more complex models that do not lend themselves to the insightful simplifications adopted here. Nevertheless, the observations made here will be validated with planned experiments.

APPENDIX I: JACOBIAN MATRICES

Jacobian Matrix for 3rd order system:

$$J = \begin{bmatrix} 0 & 1 & 0 \\ -\frac{K_T}{J_r} & J_{22} & J_{23} \\ 0 & J_{32} & J_{33} \end{bmatrix}$$

$$\begin{aligned} J_{22} = {} & \frac{F_Z R^2(\sigma_2 - \sigma_1) - C_T}{J_r} - \frac{F_Z R \sigma_0 \sigma_1}{J_r}\bar{x}_3[\Phi(\bar{x}_2)] \\ & - \frac{F_Z R^2 \sigma_1 k}{J_r}\bar{x}_3\left(\frac{\partial|\bar{x}_2|}{\partial \bar{x}_2}\right) \\ & - \frac{F_Z R \sigma_1}{J_r}\left[\mu_c + (\mu_s - \mu_c)e^{-\left(\frac{v_v}{v_s}\right)^\alpha}\right][\Phi(\bar{x}_2)] \\ & - \frac{F_Z R^2 \sigma_1 k}{J_r}\frac{\left[\mu_c + (\mu_s - \mu_c)e^{-\left(\frac{v_v}{v_s}\right)^\alpha}\right]}{\sigma_0}\left(\frac{\partial|\bar{x}_2|}{\partial \bar{x}_2}\right) \end{aligned}$$

$$\begin{aligned} J_{23} = {} & \frac{F_Z R \sigma_0}{J_r} - \frac{F_Z R \sigma_0 \sigma_1}{J_r}\frac{v_v - R\bar{x}_2}{\left[\mu_c + (\mu_s - \mu_c)e^{-\left(\frac{v_v - R\bar{x}_2}{v_s}\right)^\alpha}\right]} \\ & - \frac{F_Z R^2 \sigma_1 k}{J_r}|\bar{x}_2| \end{aligned}$$

$$\begin{aligned} J_{32} = {} & -R - \sigma_0 \bar{x}_3[\Phi(\bar{x}_2)] - \left[\mu_c + (\mu_s - \mu_c)e^{-\left(\frac{v_v}{v_s}\right)^\alpha}\right][\Phi(\bar{x}_2)] \\ & - kR\bar{x}_3\left(\frac{\partial|\bar{x}_2|}{\partial \bar{x}_2}\right) \\ & - kR\frac{\left[\mu_c + (\mu_s - \mu_c)e^{-\left(\frac{v_v}{v_s}\right)^\alpha}\right]}{\sigma_0}\left(\frac{\partial|\bar{x}_2|}{\partial \bar{x}_2}\right) \end{aligned}$$

$$J_{33} = -\sigma_0\frac{v_v - R\bar{x}_2}{\left[\mu_c + (\mu_s - \mu_c)e^{-\left(\frac{v_v - R\bar{x}_2}{v_s}\right)^\alpha}\right]} - kR|\bar{x}_2|$$

$$\begin{aligned} & \Phi(\bar{x}_2) \\ & = -\frac{R}{\left[\mu_c + (\mu_s - \mu_c)e^{-\left(\frac{v_v - R\bar{x}_2}{v_s}\right)^\alpha}\right]} \\ & - \frac{(v_v - R\bar{x}_2)\frac{R\alpha}{v_s}\left(\frac{v_v - R\bar{x}_2}{v_s}\right)^{\alpha-1}(\mu_s - \mu_c)e^{-\left(\frac{v_v - R\bar{x}_2}{v_s}\right)^\alpha}}{\left[\mu_c + (\mu_s - \mu_c)e^{-\left(\frac{v_v - R\bar{x}_2}{v_s}\right)^\alpha}\right]^2} \end{aligned}$$

Jacobian Matrix for 5th order system:

$$J_s = \begin{bmatrix} 0 & 1 & 0 & 0 & 0 \\ -\frac{K_T}{J_r} & J_{22} & J_{23} & \frac{K_T}{J_r} & \frac{C_T}{J_r} \\ 0 & J_{32} & J_{33} & 0 & 0 \\ 0 & 0 & 0 & 0 & 1 \\ \frac{K_T}{J_w} & \frac{C_T}{J_w} & 0 & -\frac{K_T + K_{ST}}{J_w} & -\frac{C_T + C_{ST}}{J_w} \end{bmatrix}$$

APPENDIX II: TYPICAL VALUES FOR THE PARAMETERS:

Parameters	Values
$K_T\ [Nm/rad]$	53000
$C_T[Nm\cdot s/rad]$	2.5
$K_{ST}\ [Nm/rad]$	16000
$C_{ST}[Nm\cdot s/rad]$	8
$J_r[kg\cdot m^2]$	1
$J_w[kg\cdot m^2]$	0.2
$R[m]$	0.27
$L[m]$	0.2
$F_Z[N]$	2617
$\sigma_0[1/m]$	623
$\sigma_1[s/m]$	1.72
$\sigma_2[s/m]$	0

μ_s	0.75
μ_c	0.4
$v_s[m/s]$	10
α	0.75

REFERENCES

[1] P. W. A. Zegelaar, "The Dynamic Response of Tyres to Brake Torque Variations and Road Unevennesses," PhD Dissertation, Delft University of Technology, 1998.

[2] A. Sueoka, T. Ryu, T. Kondou, M. Togashi, and T. Fujimoto, "Polygonal wear of automobile tire," *JSME International Journal, Series C*, vol. 40, pp. 209-217, 1997.

[3] H.-b. Huang, Y.-J. Chiu, and X.-x. Jin, "Numerical calculation of irregular tire wear caused by tread self-excited vibration and sensitivity analysis," *Journal of Mechanical Science and Technology*, vol. 27, pp. 1923-1931, 2013.

[4] R. W. Scavuzzo, T. R. Richards, and L. T. Charek, "Tire vibration modes and effects on vehicle ride quality," *Tire Science and Technology*, vol. 21, pp. 23-39, 1993.

[5] J. Adcox, B. Ayalew, T. Rhyne, S. Cron, and M. Knauff, "Interaction of Anti-lock Braking Systems with Tire Torsional Dynamics," *Tire Science & Technology*, vol. 40, pp. 171-85, 07/ 2012.

[6] R. A. Ibrahim, "Friction-induced vibration, chatter, squeal, and chaos: Part I - Mechanics of friction," in *Winter Annual Meeting of the American Society of Mechanical Engineers, November 8, 1992 - November 13, 1992*, Anaheim, CA, USA, 1992, pp. 107-121.

[7] R. A. Ibrahim, "Friction-induced vibration, chatter, squeal, and chaos: Part II - Dynamics and modeling," in *Winter Annual Meeting of the American Society of Mechanical Engineers, November 8, 1992 - November 13, 1992*, Anaheim, CA, USA, 1992, pp. 123-138.

[8] H. Hetzler, D. Schwarzer, and W. Seemann, "Analytical investigation of steady-state stability and Hopf-bifurcations occurring in sliding friction oscillators with application to low-frequency disc brake noise," *Communications in Nonlinear Science and Numerical Simulation*, vol. 12, pp. 83-99, 02/ 2007.

[9] Y. Li and Z. C. Feng, "Bifurcation and chaos in friction-induced vibration," *Communications in Nonlinear Science and Numerical Simulation*, vol. 9, pp. 633-47, 12/ 2004.

[10] X. Yang, S. Zuo, L. Lei, X. Wu, and H. Huang, "Hopf bifurcation and stability analysis of a non-linear model for self-excited vibration of tire," in *2009 IEEE Intelligent Vehicles Symposium (IV), 3-5 June 2009*, Piscataway, NJ, USA, 2009, pp. 843-7.

[11] S. K. Clark, R. N. Dodge, and G. H. Nybakken, *An evaluation of string theory for the prediction of dynamic tire properties using scale model aircraft tires*: National Aeronautics and Space Administration, 1972.

[12] J. P. Maurice, "Short Wavelength and Dynamic Tyre Behaviour Under Lateral and Combined Slip Conditions," PhD Dissertation, Delft University Press, 2000.

[13] A. J. C. Schmeitz, I. J. M. Besselink, and S. T. H. Jansen, "TNO MF-SWIFT," *Vehicle System Dynamics*, vol. 45, pp. 121-137, 2007/01/01 2007.

[14] S. T. H. Jansen, P. W. A. Zegelaar, and H. B. Pacejka, "The influence of in-plane tyre dynamics on ABS braking of a quarter vehicle model," in *Advanced Vehicle Control (AVEC) 1998, 1998*, Netherlands, 1999, pp. 249-61.

[15] J. P. Pauwelussen, L. Gootjes, C. Schroder, K. U. Kohne, S. Jansen, and A. Schmeitz, "Full vehicle ABS braking using the SWIFT rigid ring tyre model," *Control Engineering Practice*, vol. 11, pp. 199-207, 2003.

[16] A. J. C. Schmeitz, S. T. H. Jansen, H. B. Pacejka, J. C. Davis, N. M. Kota, C. G. Liang, *et al.*, "Application of a semi-empirical dynamic tyre model for rolling over arbitrary road profiles," *International Journal of Vehicle Design*, vol. 36, pp. 194-215, 2004.

[17] H. Pacejka, *Tyre and Vehicle Dynamics*: Elsevier Science, 2005.

[18] M. Gipser, "FTire: a physically based application-oriented tyre model for use with detailed MBS and finite-element suspension models," *Vehicle System Dynamics*, vol. 43, pp. 76-91, / 2005.

[19] M. Gipser, "FTire - The tire simulation model for all applications related to vehicle dynamics," *Vehicle System Dynamics*, vol. 45, pp. 139-151, 2007.

[20] E. Velenis, P. Tsiotras, C. Canudas-De-Wit, and M. Sorine, "Dynamic tyre friction models for combined longitudinal and lateral vehicle motion," *Vehicle System Dynamics*, vol. 43, pp. 3-29, 2005.

[21] C. Canudas de Wit, H. Olsson, K. J. Astrom, and P. Lischinsky, "A new model for control of systems with friction," *IEEE Transactions on Automatic Control*, vol. 40, pp. 419-25, 03/ 1995.

[22] C. Canudas-de-Wit, "Comments on 'a new model for control of systems with friction'," *IEEE Transactions on Automatic Control*, vol. 43, pp. 1189-1190, 1998.

[23] K. Johanastrom and C. Canudas-de-Wit, "Revisiting the LuGre friction model," *Control Systems, IEEE*, vol. 28, pp. 101-114, 2008.

[24] L. Freidovich, A. Robertsson, A. Shiriaev, and R. Johansson, "LuGre-model-based friction compensation," *IEEE Transactions on Control Systems Technology*, vol. 18, pp. 194-200, 2010.

[25] C. Yan and W. Junmin, "Adaptive Vehicle Speed Control With Input Injections for Longitudinal Motion Independent Road Frictional Condition Estimation," *IEEE Transactions on Vehicular Technology,* vol. 60, pp. 839-48, 03/ 2011.

[26] J. Adcox and B. Ayalew, "ADAPTIVE TRACTION CONTROL FOR NON-RIGID TIRE-WHEEL SYSTEMS," in *ASME 2013 Dynamic Systems and Control Conference, DSCC2013, October 21-23, 2013*, Palo Alto, California, USA, 2013.

[27] J. Guckenheimer and P. Holmes, *Nonlinear Oscillations, Dynamical Systems, and Bifurcations of Vector Fields*: Springer-Verlag, 1997.

[28] S. H. Strogatz, *Nonlinear Dynamics and Chaos: With Applications to Physics, Biology, Chemistry, and Engineering*: Westview Press, 2008.

[29] H. Olsson, K. J. Astrom, C. Canudas de Wit, M. Gafvert, and P. Lischinsky, "Friction models and friction compensation," *European Journal of Control*, vol. 4, pp. 176-95, / 1998.